Dytran by HBK
HOTTINGER BRÜEL & KJÆR

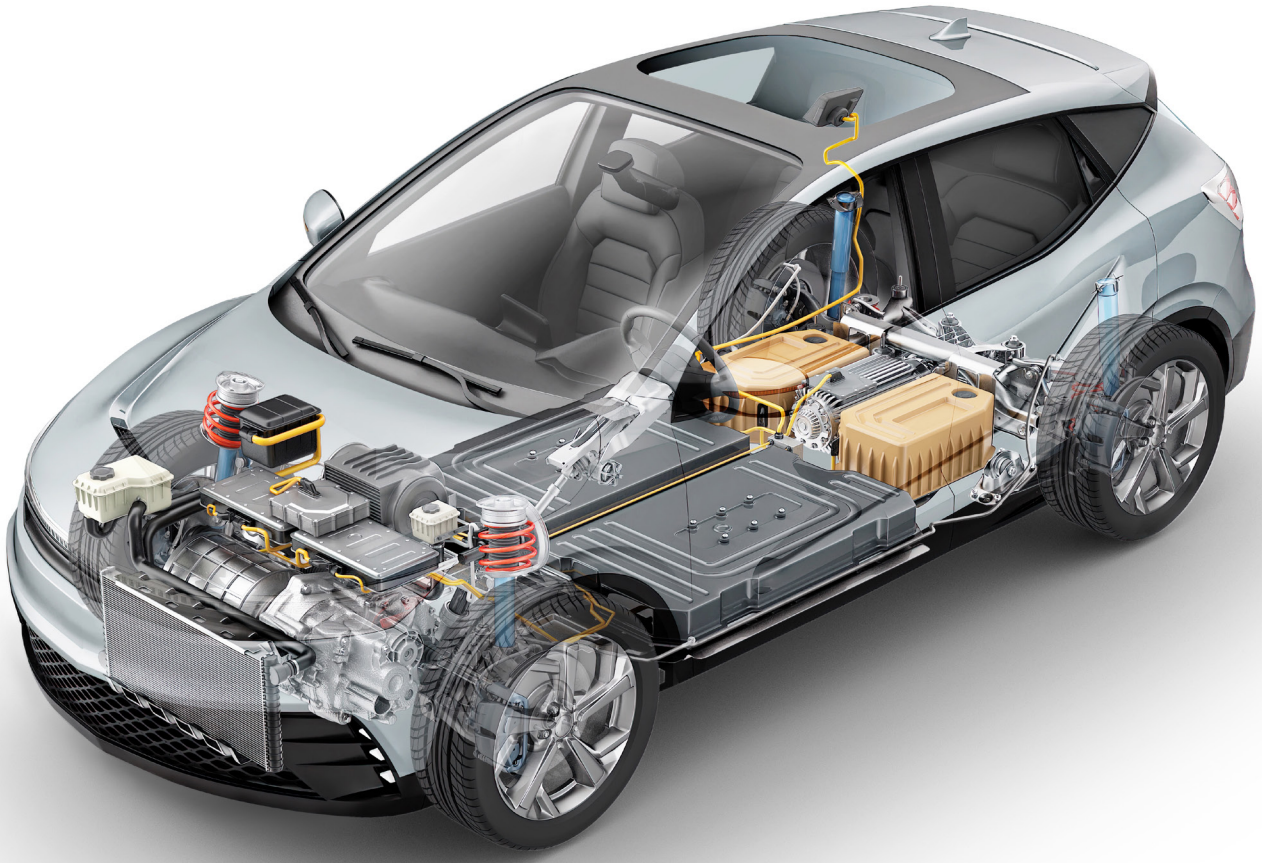

WHITE PAPER

Sensing technology and electrical interface selection for areas with high EMI/RFI intensity

Author: Brian Johnson
Applications Development Supervisor
Dytran by HBK

TABLE OF CONTENTS

1. INTRODUCTION

The foundation of any development, improvement, or progress in the modern world requires a baseline measurement for comparison to future results. This baseline is established through initial measurement of the current state of a technology, and subsequent modifications must also be measured to determine progress (or lack thereof). Sensors and sensing technologies are essential in establishing these baselines and determining continuous growth. As such, they will continue to play a crucial role in the development cycle.

Selecting the appropriate sensor and sensing technology for a measurement task can be challenging due to the multitude of options available. This selection process becomes even more complex when dealing with EMI/RFI (Electromagnetic Interference/Radio Frequency Interference), which can alter, disrupt, or interfere with electrical signals. Digital technologies possess safeguards against EMI/RFI, but analog signals remain vulnerable. The rise in electric vehicles has led to increased EMI risks in environments with high switching and induction currents. In analog measurements, real-time signal accuracy verification is not possible, making EMI/RFI an even greater concern.

The purpose of this paper is to examine the susceptibility of various prominent sensing technologies and electrical interfaces to EMI/RFI. It is crucial to note that the effects of EMI/RFI depend heavily on factors such as installation, cable length, and DAQ system specifics. This experiment will compare the performance of different vibration sensor technologies under similar conditions.

An initial survey was conducted to determine the frequency range which would yield the highest susceptibility to EMI across various sensor types. The testing was performed within a frequency range of 30 MHz to 1 GHz. Figure 1 below illustrates the findings of this preliminary survey.

The most significant disturbance was observed at the EMI/RFI frequencies between 250 MHz and 600 MHz. The amplitude of the emissions was adjusted to approximately 35 V/m throughout the frequency range. This selection was attained by gradually increasing the emission levels until the UUT (unit under test) with the lowest susceptibility began displaying a disturbance due to EMI. Once the test conditions were established, various sensors were subjected to the same 0.95 interference levels and the effects were recorded using a data acquisition system.

All UUTs exhibited some level of signal degradation from EMI during the test. The extent of signal degradation was evaluated based on the amplitude of the interference, duration of the disturbance, and the user's ability to restore the state of the true vibration signal. Each sensing technology and electrical interface was graded in accordance with its EMI/RFI susceptibility. The results and conclusions are described in the sections below, accompanied by a brief description of each sensor and an explanation of their internal operation.

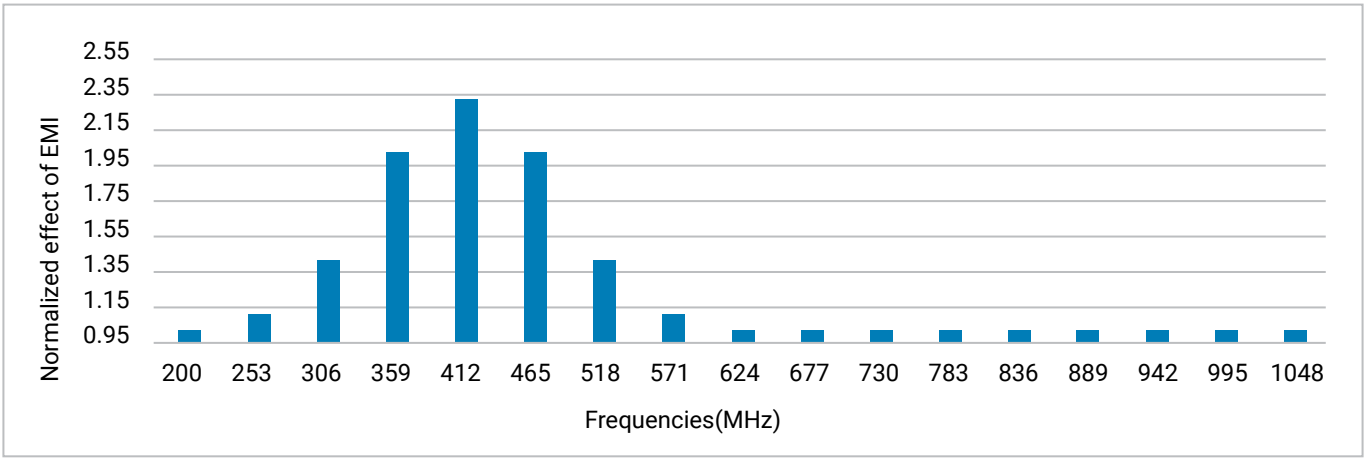

Figure 1: Frequencies with highest EMI effect (empirical results)

1.1 RESULTS AND CONCLUSIONS

The table below ranks the tested sensor technologies in descending order of susceptibility. A higher susceptibility rating indicates that the UUT is more influenced by EMI/RFI signals making it less desirable for use in high EMI environments. Based on the results presented, the CVLD electrical interface with MEMS sensing technology appears to be the best choice for an analog sensor. Meanwhile, digital solutions undoubtedly demonstrate near to absolute immunity to EMI/RFI susceptibility.

Table 1: Sensor technology and electrical interface ratings in relation to electromagnetic immunity (the lower the rating the better the immunity)

EMI/RFI Susceptibility Rating	Sensing Technology	Electrical Interface	Comments
10	Piezoelectric (piezoceramic)	IEPE (Charge Amplifier)	Charge amplifiers, when used in conjunction with piezoelectric ceramics, can provide exceptional levels of resolution and signal quality. Highly sensitive piezoelectric materials, combined with extremely low-noise electronics, push the sensor's dynamic range to impressive levels of 105 – 110 dB. However, this performance comes at a cost: if not designed specifically for EMI/RFI, these circuits may be unstable under such conditions. IEPE charge amplifiers employ a negative feedback mechanism for bias voltage balancing, and any interference can disrupt this balance, leading to signal discrepancies. To mitigate the effects of EMI/RFI the user should ensure that circuits have adequate protection.
9	Piezoelectric (piezoceramic or single crystals)	Charge	Electrical charge, being the most delicate signal carrier, is particularly susceptible to external EMI/RFI. It is imperative to keep the charge mode cables as short as possible. Extreme temperature environments are the primary reason for using this technology. As soon as temperature conditions permit, users should place a charge amplifier with adequate protection in line with the signal cable to reduce the impedance level.
8	Piezoelectric (single crystals)	IEPE (Impedance Converter)	Impedance converter circuits are typically used with single crystal piezoelectric materials, such as quartz or langatate. These circuits usually consist of a single semiconductor and, unlike charge amplifiers, do not require self-balancing negative feedback to maintain proper bias voltage. On one hand, this simplicity makes the circuits more likely to withstand EMI/RFI effectively. On the other hand, it makes it impossible to amplify the signal levels within the amplifier (which is why impedance converters are also known as gain of one amplifier). Generally, these circuits have inferior resolution compared to their piezoceramic charge amplifier counterparts.
7	Variable capaci-tance, MEMS	4-wire Differential Signal	The 4-wire interfaces introduce additional complexity to the measurement chain due to the increased number of conductors. However, the presence of a pair of signal wires allows users to employ common mode rejection techniques, which help mitigate some of the EMI/RFI effects.

6	Piezoelectric (quartz)	CVLD	CVLD technology uses an electrical current rather than voltage to transmit measurement signals. EMI has more difficulty affecting a signal carried by an electrical current, as it only induces a tiny amount of electrical current onto the signal cable. For a CVLD sensor, the induced current on the cable is insignificant compared to the signal current. In contrast, for a voltage mode sensor the same small amount of current injected by EMI can create a significant voltage level once it passes through the high input impedance of the DAQ. Important note: The UUT tested for this paper was specifically designed for cryogenic applications, which significantly increased the complexity of the circuitry. By implementing additional design considerations, its EMI/RFI susceptibility could be further improved, bringing it closer to its MEMS counterpart.
5	Piezoelectric (piezoceramic)	IEPE (Charge Amplifier with EMI Suppression)	When the potential issue of EMI/RFI interference is effectively addressed in the design of an IEPE charge amplifier, it can offer the optimal combination of high dynamic range and EMI/RFI resistance. The new Dytran by HBK 3055/3056F series successfully addresses this aspect of operation.
4	Variable capacitance, MEMS	CVLD	Dytran by HBK offers several families of MEMS-based CVLD sensors. The combination of these two technologies appears to provide a superior sensing solution, offering adequate frequency response, dynamic range, two-wire connection simplicity, and a robust design.
3	Variable capacitance, MEMS	3-wire Single ended Signal	The test results for Dytran by HBK sensor family 7531/7533 were a surprising discovery. This type of sensor is considered inferior to other sensors tested in this study in terms of resolution and frequency response. However, it demonstrated the most robust EMI immunity among the analog sensor group. On average, these sensor families demonstrate a relatively modest dynamic range of roughly 43 dB and frequency response of just over a kilohertz. Combined with a fairly high output impedance of 32 kOhm, which typically prevents long cable runs, and budget-conscious packaging (these sensors are not hermetically sealed and feature an anodized aluminum housing), they would be an unlikely selection for demanding applications.
2	Variable capacitance, MEMS or piezoelectric	CAN	The CAN-MD® sensors used in this test feature a digital CAN bus output. Since the analog signal remains within the sensor housing and all the conditioning and analog to digital conversions occur inside a shielded enclosure, it is logical that this type of a device would exhibit superior performance in EMI/RFI environments. The Dytran 3495 series used in this test is a miniaturized member of the CAN-MD family. Due to the size constraints, the sensing element is positioned very close to the computational electronics within the sensor housing, but it does not share the same Faraday shield with the digital board. This arrangement leaves the short analog line (which does not exceed a quarter of an inch) exposed to a potential EMI risk. However, the test results indicate that this compromise has a minimal effect on the sensor readings.

1	Variable capacitance, MEMS or piezoelectric	CAN	The Dytran 3410A CAN-MD® sensor is a state-of-the-art digital accelerometer that features a robust and well-protected design. Its internal construction enables proper shielding of all electronic components, including the internal analog signal lines. This approach completely resolves the issue of EMI/RFI interference, and the test results show a signal record that remains entirely unaffected by the generated interference.

1.2 SENSING TECHNOLOGIES AND ELECTRICAL INTERFACES

The following sections detail the sensing technologies evaluated in this test, including their electrical interfaces and principles of operation. The diagram representations include a depiction of the grounding schema for each of the sensor types during the tests. It is important to note that all the sensors had some variation of ground isolation (either case isolation or base isolation). For environments with potential EMI/RFI or ground loop risks, it is strongly recommended to use only isolated sensors. The descriptions below include the Dytran model numbers used for the tests and discuss some options that users may have within a given technology to potentially enhance its immunity to electromagnetic signals.

1.2.1 PIEZOELECTRIC CHARGE MODE

Charge mode piezoelectric sensors are the oldest technology tested. Their initial simplicity of use and absence of complex electronics made these types of sensors extremely popular among users. At the core of this technology is a piece of a piezoelectric material (crystal or a crystalline material with asymmetric lattice structure) that generates an electric charge on its surface in response to physical force. This charge response is almost linear with respect to the physical measurand. The sensors typically require only two connections (positive and negative/ground) and have a very high reliability due to the minimal number of components. Such simplicity, however, comes at a cost. The charge developed by the sensor is a fragile signal carrier susceptible to various environmental disturbances. Triboelectric cable noise, high insulation resistance requirements, and the need for a charge amplifier are just some of the challenges users must overcome when using this technology. The schematic diagram below shows the implementation of this technology during the test. The model number of the sensor is 3055C, the charge amplifier is 4754B1, the sensor to the charge amplifier cable is 6013A and the charge amplifier to the DAQ system connection used a 6019A cable. As mentioned above, the sensor and the signal line were ground isolated. During the test, all items except the sensor and the coaxial cable between the sensor and the charge amplifier were shielded.

Despite all its shortcomings, this technology continues to thrive in environments with extreme temperature requirements and numerous legacy applications that have infrastructures specifically configured for this type of sensor.

The main reason this technology is susceptible to e lectromagnetic influence is that electromagnetic interference (EMI) injects miniscule amounts of electrical current into the signal wires. An electrical current is defined as the flow of electrical charge over time, which is the same carrier used to transmit the actual signal in this technology. As a result, the signal created by EMI becomes indistinguishable from the signal created by the measurand. Despite the EMI frequency being much higher than the frequency created by the measurand, its disturbance is still capable of creating spurious artifacts.

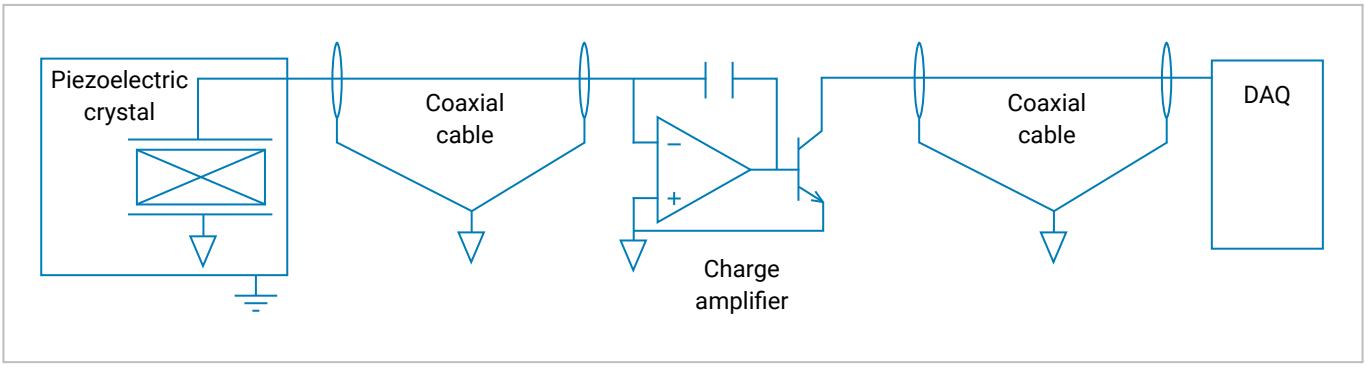

Figure 2: Schematic representation – Charge Mode System

1.2.2 PIEZOELECTRIC IEPE (CHARGE AMPLIFIER WITH PIEZOCERAMIC)

The IEPE acronym stands for Internal Electronics Piezoelectric. This technology utilizes the concepts described in the previous section, but it complements the piezoelectric sensing element with a miniature electrical circuit placed inside the sensor. This circuit converts the charge output produced by the crystal into a low-impedance voltage signal. As a result, the signal is more tolerant to triboelectric noise and long cable runs, and it can be easily interpreted by most data acquisition systems used for sound and vibration measurements.

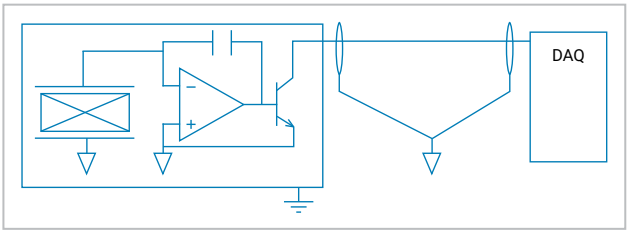

Figure 3: Schematic representation – IEPE Charge Amplifier

The model numbers used in this test were the Dytran sensor model 3055D11 and cable model 6013A. The sensor model 3055D11 is ground isolated using an off-ground base. The popularity of this design is explained by the convenience of use. These sensors are used with coaxial cables, where the center conductor is referred to as “Signal/Power” line, and the outer shield works as the ground return. The center conductor both powers the sensor and extracts the electrical signal. To accomplish this, the sensor is powered by a supply with a constant limited current typically ranging from 2 to 20 mA and a compliance voltage of 18 to 30 VDC. Once the sensor is connected to the power supply, the compliance voltage drops to the bias voltage (typically 7 to 13 VDC) due to the current limitation. The bias voltage is equivalent to a measurand of zero and is internally maintained by the sensor electronics, regardless of the actual supply current, as long as it remains within the specified constant current and compliance voltage range. While the bias voltage generally remains roughly in the middle of the compliance range, it has the ability to decrease (to express the negative swing of the measurand) or increase (to express the measurand’s positive swing). Since this technology is primarily used for dynamic measurements, the precise value of the bias voltage is not crucial, and the DC component is typically filtered out using a coupling capacitor.

The main reason this technology is susceptible to EMI is the bias voltage. High-intensity radio signals have a tendency to disrupt the state of the bias voltage, and while the amplifier attempts to restore the bias, it can be misinterpreted as an actual signal by the DAQ. Without proper measures to mitigate this effect, the bias voltage will start fluctuating. These spurious fluctuations manifest as an increase in amplitude at low frequencies, commonly referred to as a “ski slope” effect in the frequency domain. There are design considerations that can help improve the EMI susceptibility of these circuits; however, they typically result in an overall increase in the size of the sensor.

1.2.3 PIEZOELECTRIC IEPE (CHARGE AMPLIFIER WITH EMI SUPPRESSION PIEZOCERAMIC)

Similar to the sensors discussed in the previous section, IEPE charge amplifiers with internal EMI suppression utilize internal electronics to self-adjust their bias voltage. However, an important addition to the design is the RF suppression components, typically installed at the signal/power end of the amplifier, as shown in the diagram below.

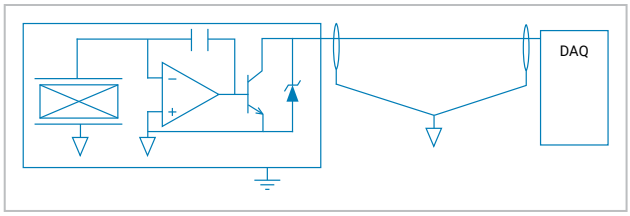

Figure 4: Schematic representation – IEPE Charge Amplifier with EMI Suppression

The suppression components typically consist of diodes, capacitors, or resistors arranged in a specific network. These components work together to suppress high-frequency energy before it enters the amplifier and disturbs the bias voltage. Consequently, the bias voltage remains stable, providing an unaltered output of the electrical signal.

To demonstrate the EMI suppression capability, the brand new Dytran series 3055/3056F was used. This series utilizes a new low-noise, high-temperature charge amplifier with built-in EMI suppression. Despite being exposed to mild levels of EMI/RFI, this charge amplifier can deliver a dynamic range of 105 – 110 dB while staying relatively unaffected by mild levels of EMI/RFI.

1.2.4 PIEZOELECTRIC IEPE (IMPEDANCE CONVERTER WITH QUARTZ CRYSTALS)

Another type of IEPE sensor technology utilizes quartz crystals as its piezoelectric material, as opposed to piezoceramic crystals. These sensors employ an impedance converter for their IEPE electronics. While the impedance converter (also known as a gain of 1 amplifier) operates according to the same IEPE specifications (2 – 20 mA current, 18 – 30 VDC compliance) as described in the previous section about IEPE charge amplifiers, the user may not realize the difference in the internal electronics. Typically, impedance converters are used with quartz-based sensors, while charge amplifiers are used with piezoceramic crystals. The impedance converter is a simpler circuit compared to an IEPE charge amplifier. It typically relies on a single semiconductor, most commonly a P-channel MOSFET, to establish the bias voltage and transmit the signal. The internal properties of the semiconductor function similar to a Zener diode in determining the bias voltage. This schema is more robust as it lacks negative feedback that could be disturbed by EMI. Consequently, impedance converters perform quite well in EMI environments, even without the presence of suppression components. Quartz material exhibits exceptional stability over a wide range of temperatures (–420°F to 500°F), making it well-suited for use in airborne or space applications. The 3168 series used for this experiment is one of the most popular models for such applications.

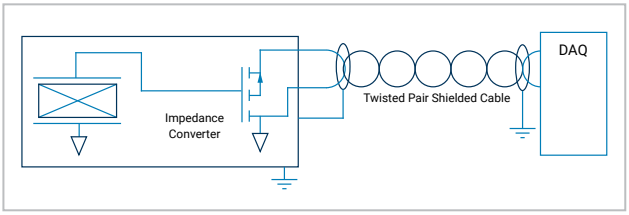

Figure 5: Schematic representation – IEPE Impedance Converter

Another important aspect of these installations was the use of twisted pair shielded cables. Typically, these cables offer greater robustness against EMI/RFI interference. This can be attributed to the symmetry of the conductors within the electromagnetic medium. In other words, any electromagnetic disturbance affects both conductors at the same time, resulting in virtually no electronic potential between them. Since one of these conductors serves as the signal/power line and the other as the ground return, any interference that shows up as a disturbance must appear in between those two wires in the form of an electric potential.

1.2.5 DC MEMS WITH DIFFERENTIAL OUTPUT

Another type of sensing technology available on the market is variable capacitance sensors. Unlike their piezoelectric counterparts, sensors of this type can measure steady-state events. While piezoelectric sensors can only measure changes in a measurand, eventually decaying to zero if the measurand remains constant, variable capacitance sensors operate based on the principle of changing capacitance. The sensing element contains a moving metallic plate that bends freely under the forces of inertia in relation to the stationary plates. As the distance between the moving and stationary plates changes, the capacitance also changes. The circuitry inside the sensor continuously converts the change in capacitance into a voltage. The voltage equivalent of the capacitance becomes the output signal. Some variable capacitance sensors feature a differential output, which enhances EMI/RFI immunity by utilizing the common mode rejection effect.

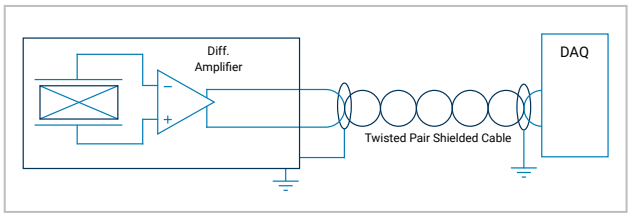

Figure 6: Schematic Representation – DC MEMS, Differential

The circuitry used in variable capacitance sensors is more complex than that of piezoelectric sensors. These MEMS sensors typically come at a higher cost and larger size compared to piezoelectric sensors with comparable performance specifications. The integration and troubleshooting process can also be more complex due to the wiring involved. However, the most significant advantage of variable capacitance sensors is their ability to measure 0 Hz acceleration due to gravity. While piezoelectric sensors can potentially provide responses at very low frequencies, the intrinsic capability of MEMS technology to reach 0 Hz makes it the de facto standard for low-frequency measurements.

1.2.6 DC MEMS WITH SINGLE-ENDED OUTPUT

DC MEMS sensors with single-ended output operate on the same principle as described above; however unlike its differential counterpart they only have one output line. Theoretically, this could make a sensor more susceptible to EMI. However, the test results demonstrate the opposite effect. It is important to note that the single-ended MEMS sensor used in this experiment has inferior specifications compared to the other sensors tested. Some of its shortcomings actually contribute to its reduced susceptibility to EMI. For example, the output impedance of the sensor is approximately 32 kOhm, which is significantly higher compared to the 2 – 100 Ohm output impedances of other devices mentioned in this article. This high output impedance requires the DAQ to have an extremely high input impedance to operate properly. Additionally, the high output impedance makes the signal line more susceptible to in-band interference, which refers to EMI that is present within the frequency band of measurement (in this case under 1000 Hz). This explains why a 60 Hz signal is clearly visible in the test results.

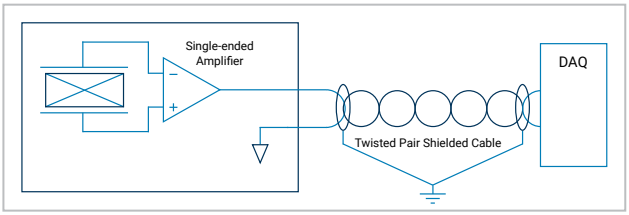

Figure 7: Schematic Representation – DC MEMS, Single Ended

The high output impedance prevents the use of long cable runs used in the installation of this sensor. With longer cable runs, it becomes increasingly challenging for a sensor with high output impedance to maintain the voltage levels associated with the acceleration signal. In addition, sensors of this type typically display higher noise levels.

1.2.7 PIEZOELECTRIC CVLD

The CVLD abbreviation stands for Constant Voltage Line Driver. It implies that during the signal transition from high to low, the voltage level stays constant while the current changes proportionally to the variation of the measurand. At the receiving end of the DAQ, the signal current passes through a sense resistor, generating a voltage which is recorded by the DAQ. Typically, the values of the sense resistors used are typically low and range between 5 and 100 Ohms.

This technique of signal broadcasting is robust against EMI/RFI. This approach excels because EMI/RFI signals only inject a small amount of current into the sensor cable. When the signal is carried by voltage, as is the case with IEPE devices, the small amount of current injected by EMI, when passing through the input and output impedance combination of the network, can create a significant voltage that distorts the signal. However, when the signal is carried as a current, the current injected by EMI is not significant enough compared to the amount generated by the “useful” signal.

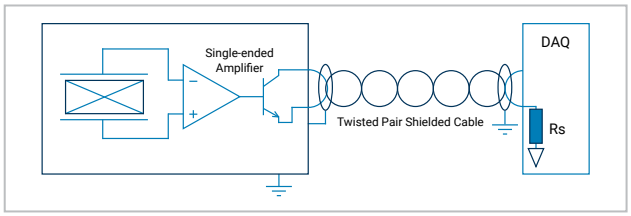

Figure 8: Schematic Representation – CVLD, Piezoelectric

The CVLD interface can be used by various sensing technologies. Dytran is developing several models that combine piezoelectric sensing technology with the CVLD protocol.

1.2.8 DC MEMS CVLD

The concept of the MEMS-based CVLD sensor is very similar to the piezoelectric CVLD sensor described above, with the only difference being the sensing technology used. This combination provides users with the EMI immunity of CVLD along with the DC response of a variable capacitance MEMS sensor.

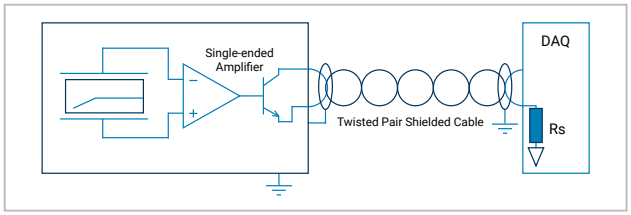

Figure 9: Schematic Representation – CVLD, MEMS

1.2.9 DIGITAL OUTPUT SENSOR (CAN-BUS BASED ACCELEROMETERS)

The CAN-MD® sensors, unlike the analog sensors described earlier in this test, use a digital communication protocol to transmit vibration data. The CAN-MD® sensors employ a piezoelectric element similar to the ones previously discussed, but instead of transmitting the analog signal over a long cable to a DAQ, the sensor conducts the analog-to-digital conversion internally.

Additionally, the sensor includes an embedded microcontroller that conducts analysis on the vibration signal. Features are extracted from the vibration signal, and the processed data (Condition Indicator) is transmitted over the CAN bus (Controller Area Network).

CAN-bus based sensors demonstrate greater resistance to electromagnetic interference compared to analog sensors for several reasons. Firstly, the CAN-MD® sensors use a twisted pair of wires in a multi conductor shielded cable that provides a high level of protection from external electromagnetic fields. This shielding helps prevent EMI from interfering with the signals transmitted between the sensors and the controller. Secondly, the sensors use a digital signal to transmit data, which is inherently less susceptible to EMI compared to analog signals. Digital signals have defined voltage levels and transition times, making them less prone to being affected by external electromagnetic fields. Finally, the CAN protocol includes error detection and correction mechanisms, ensuring that the data transmitted between the sensors and the controller is accurate, even in the presence of EMI.

Overall, these factors make CAN bus sensors less susceptible to EMI compared to analog sensors, making them a reliable and robust choice for applications where high EMI can be a concern.

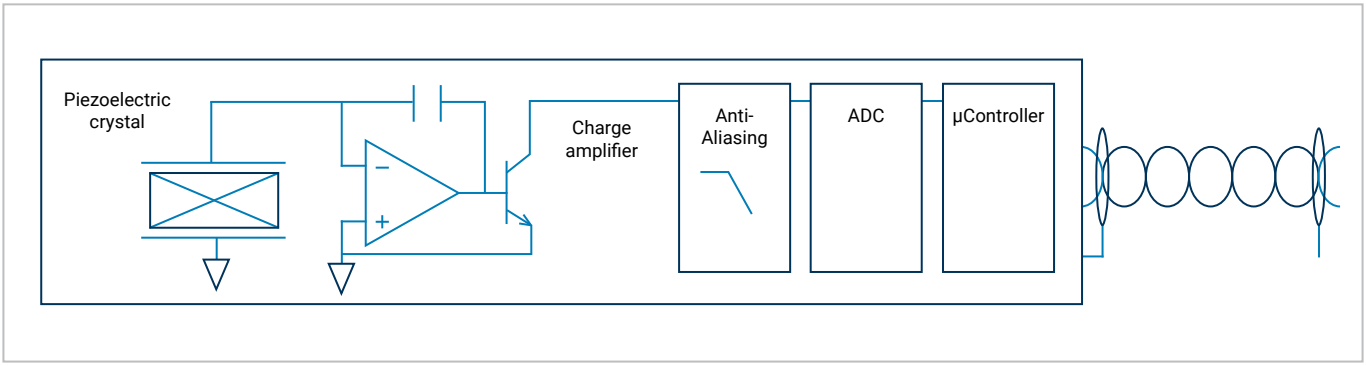

Figure 10: Schematic Representation – Digital Architecture

2. TEST SETUP AND DESCRIPTION

An EMI susceptibility test requires the use of specialized equipment, including a signal generator, amplifier, antennas, and an EMI receiver. The signal generator is used to produce the EMI signals at the appropriate frequencies. This signal is then fed into a high-power amplifier to reach the required amplitudes for the test. A transmitting antenna designed for the tested frequency band being tested is used to emit the signal into the surrounding environment. A receiving antenna connected to an EMI receiver is utilized to measure the level of EMI present in the environment.

These components were used to establish a controlled EMI environment in which various sensor technologies could be evaluated. The diagram and accompanying overview photo below illustrate the test setup with the aforementioned test hardware.

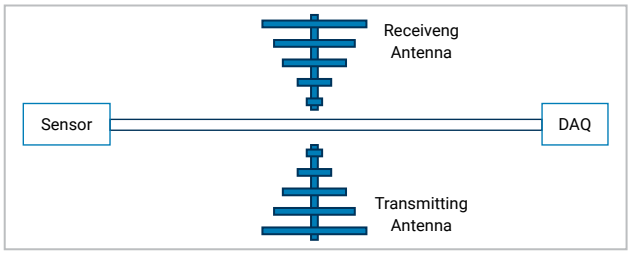

Figure 11: Schematic Representation – Test Setup

Figure 12: Actual Image – Test Setup

2.1 EMI/RFI GENERATION

The EMI signal was generated using a high-frequency signal generator programmed to sweep through frequencies between 200 MHz and 1 GHz. The output of the signal generator was fed through a high-power amplifier to adjust the signal's amplitude to approximately 30 V/m after being emitted by the transmission antenna. The images below show the EMI generation hardware and the signal generator settings.

Figure 13: Actual Image – EMI/RFI Generation

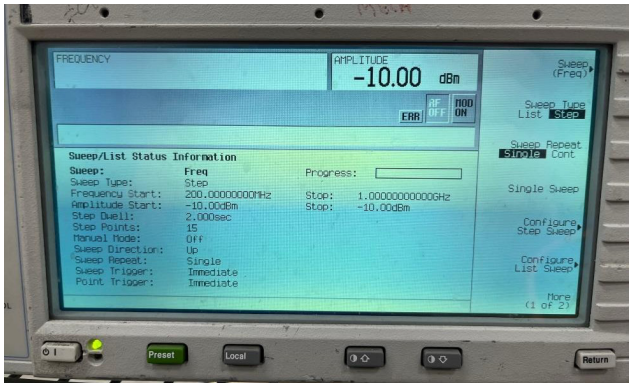

Figure 14: Actual Image – Function Generation Settings

2.2 SENSOR EXCITATION

During each sensor evaluation, the unit under test was connected to an electrodynamic shaker, which provided a sinusoidal vibration stimulus of 1 Grms at 100 Hz. The fluctuations in the sensor's output resulting from this input level allowed for the evaluation of the effects on the signal during normal operation of each sensor technology. The image below depicts the sensor excitation setup employed during the testing process.

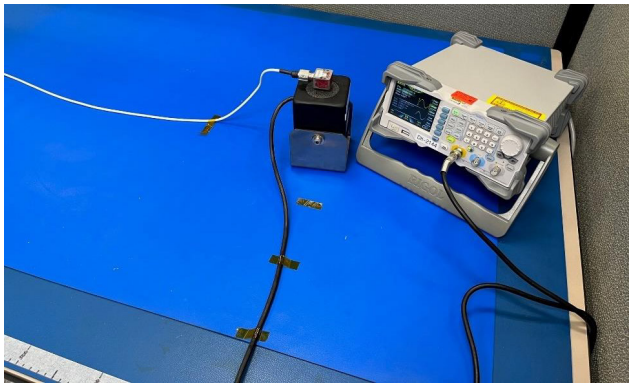

Figure 15: Actual Image – Sensor Excitation

2.3 DATA ACQUISITION

In this test, a data acquisition system was used to capture the output from all the analog sensors. This particular data acquisition system utilizes a universal connection port that, when paired with the appropriate front-end adapter, allows for the connection to the various sensor technologies.

To mitigate the impact of EMI on the data acquisition unit itself, the system was shielded within a grounded metal enclosure during testing.

The CAN-MD® sensors were the only units tested that did not connect to the DAQ. Instead, the CAN bus messages were captured by a PC using a CAN to USB interface adapter.

3. TEST RESULTS AND DISCUSSION

The following results depict the output from each sensor technology when exposed to the same EMI environment. Each recording was synchronized with the start of the EMI frequency sweep at 200 MHz and concluded after the end of the sweep at 1 GHz. This synchronization allows for comparisons of susceptibility levels among different sensor types and identifies the EMI frequencies with the most significant impact.

The plots we will focus on are the running time domain plots, which illustrate shifts in the nominal input vibration signal, and the waterfall plots, which demonstrate how these changes in the time domain affect the data in the frequency domain.

3.1 CHARGE MODE ACCELEROMETER

In the data obtained from the charge mode accelerometer, noticeable saturation events can be observed in the time domain plots. This saturation is characterized by a spike in output followed by an asymptotic decay as the amplifier discharges from a saturation event. These saturation events are a strong indicator that this sensor technology is highly susceptible to the EMI environment used in the test. The saturation event can also be observed in the waterfall plot, represented by a characteristic ski-slope output. The amplitude of the low frequency in the sensor output significantly increases because of the saturation and changing bias.

Furthermore, it is worth noting that the sensor does not exhibit this effect across the full frequency range of the test. The range of greatest susceptibility appears to be between 500 and 800 MHz.

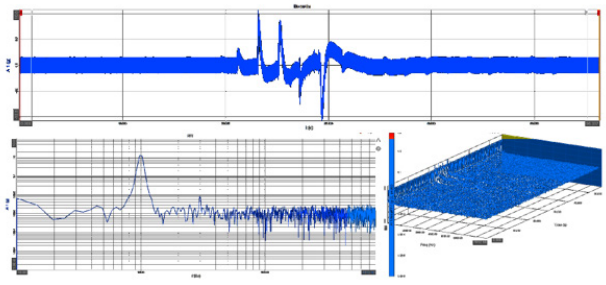

Figure 16: Software Image – Charge Mode Accelerometer Results

3.2 IEPE PIEZOELECTRIC CERAMIC ACCELEROMETER

In the data obtained from the IEPE piezoelectric ceramic accelerometer, significant saturation events can be observed in the time domain plots. These saturation events are also apparent in the waterfall plot, displaying the characteristic ski-slope.

Similar to the charge mode sensor, the IEPE piezoelectric ceramic accelerometer does not exhibit this effect across the full frequency range of the test. The range of greatest susceptibility appears to be between 300 and 600 MHz.

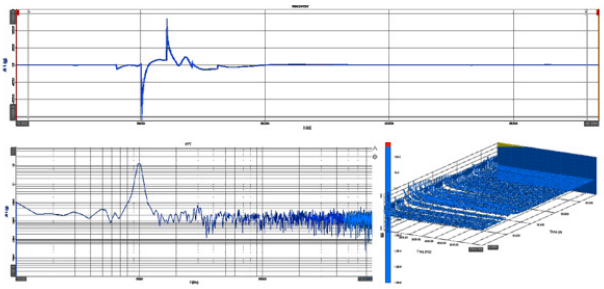

Figure 17: Software Image – IEPE Charge Amplifier Accelerometer Results

3.3 IEPE PIEZOELECTRIC CERAMIC WITH EMI SUPPRESSION ACCELEROMETER

In the data obtained from the IEPE piezoelectric ceramic accelerometer with EMI suppression, a significant reduction in the amplitude of the disturbance compared to the previous examples can be observed. Additionally, the duration between a disturbance and the sensor returning to a normal state of operation appears to be shorter. However, saturation can still be observed in the waterfall plot, represented by the characteristic ski-slope pattern.

Similar to the previous sensors, the IEPE piezoelectric ceramic accelerometer with EMI suppression does not exhibit this effect across the entire frequency range of the test. The range of greatest susceptibility for this sensor appears to be between 400 and 700 MHz.

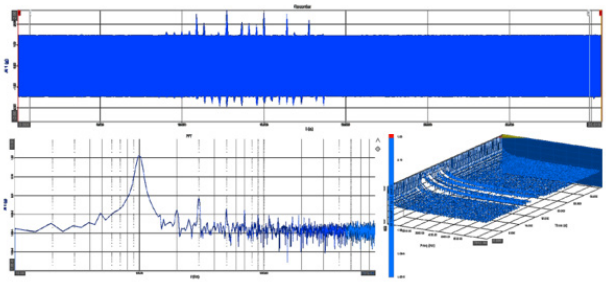

Figure 18: Software Image – IEPE Charge Amplifier with EMI Suppression Accelerometer Results

3.4 IEPE QUARTZ ACCELEROMETER

In the data acquired from the IEPE quartz accelerometer, significant amplifier saturation events can once again be observed, although the amplitude of the disturbance is greatly reduced compared to the piezoceramic sensor. As in the previous cases, saturation can be observed in the waterfall plot, indicated by the characteristic ski-slope pattern.

Similar to the other sensors, the IEPE quartz accelerometer does not exhibit this effect across the entire frequency range of the test. The range of greatest susceptibility appears to be between 400 and 700 MHz.

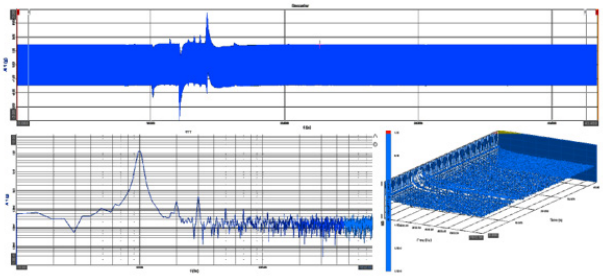

Figure 19: Software Image – IEPE Quartz Accelerometer Results

3.5 DC MEMS DIFFERENTIAL ACCELEROMETER

In the data obtained from the MEMS differential accelerometer, a significant bias can be observed in the output during the range of highest susceptibility. This shift persists almost continuously for approximately five seconds during the frequencies where the sensor is most susceptible. Saturation can still be observed in the waterfall plot, as characterized by the ski-slope-pattern and in several cases where the entire spectrum is elevated over the full bandwidth of the FFT.

Again, the sensor does not show this effect over the full frequency range of the test. The range of greatest susceptibility appears around 400 and 600 MHz.

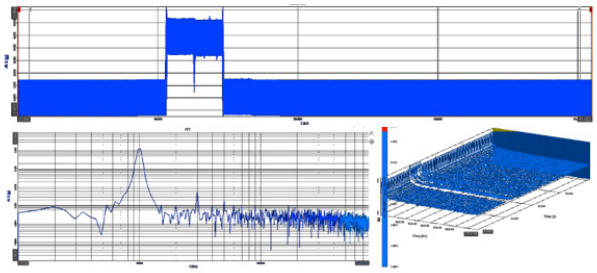

Figure 20: Software Image - DC MEMS Differential Accelerometer Results

3.6 DC MEMS SINGLE-ENDED ACCELEROMETER

The results obtained from the MEMS single-ended accelerometer were quite surprising. The sensor appears to exhibit little to no signal degradation from EMI. However, when comparing the data to the other sensors in this test, the inherent noise level of this sensor becomes apparent.

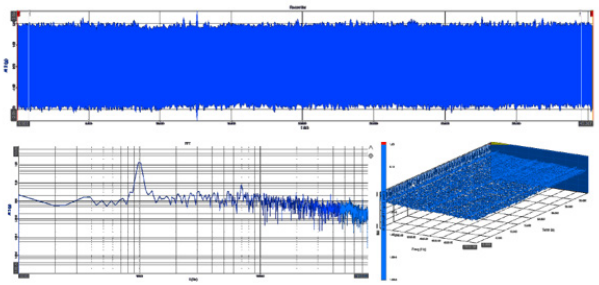

Figure 21: Software Image – DC MEMS Single-ended Accelerometer Result

3.7 CVLD PIEZOELECTRIC ACCELEROMETER

In the data obtained from the CVLD piezoelectric accelerometer, we once again observe signal degradation similar to the differential MEMS sensor. Extended durations of biased output can be seen, and saturation is still observed in the waterfall plot, indicated by the characteristic ski-slope pattern.

Like the other sensors tested, the CVLD piezoelectric accelerometer does not show this effect over the full frequency range of the test. The range of greatest susceptibility appears around 350 to 700 MHz.

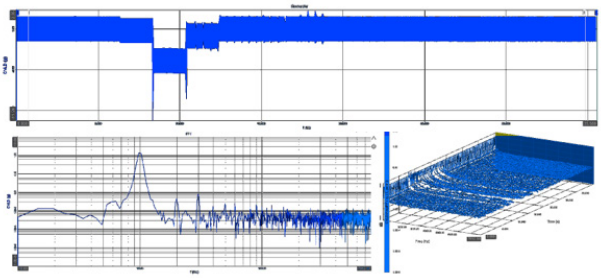

Figure 22: Software Image – CVLD Piezoelectric Accelerometer Results

3.8 CVLD MEMS ACCELEROMETER

In the data obtained from the CVLD MEMS accelerometer, we can observe a significant improvement in the output compared to the CVLD piezoelectric accelerometer. Although a bias is still present in the data as we step through the various EMI frequencies, the results show a significant improvement. In the waterfall plot, only a slight disturbance at around 30 seconds is observable.

Similar to the other sensors, the CVLD MEMS accelerometer does not display this effect over the full frequency range of the test. The range of greatest susceptibility appears around 350 to 700 MHz.

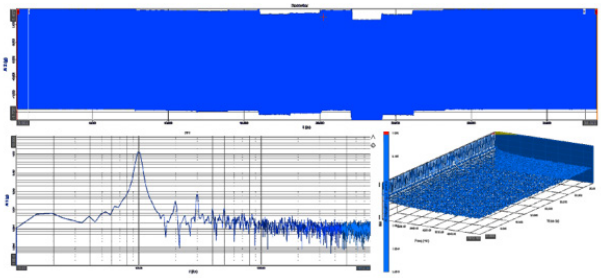

Figure 23: Software Image – CVLD MEMS Accelerometer Results

3.9 DIGITAL ACCELEROMETER – 3495A

The data from the 3495A CAN-MD® Smart Accelerometer is presented below. This particular sensor is unique in that it processes data directly within the sensor itself and outputs the analysis results over a CAN bus. As a result, it does not provide continuous time domain output but instead tracks an RMS condition indicator. Additionally, the sensor is configured to generate frequency domain plots for each acquisition, and these spectra are combined in post-processing to create the waterfall plot below.

The results obtained from the 3495A sensor demonstrate near immunity to the EMI signal. Only a small disturbance in the RMS output was observed around CI occurrence 120, which corresponds to approximately 500 MHz – the frequency range where several of the previously analyzed sensor technologies exhibited the greatest susceptibility to EMI.

The waterfall plot indicates no signs of saturation across the full frequency range tested, further confirming the robustness of the 3495A CAN-MD® Smart Accelerometer in the presence of EMI.

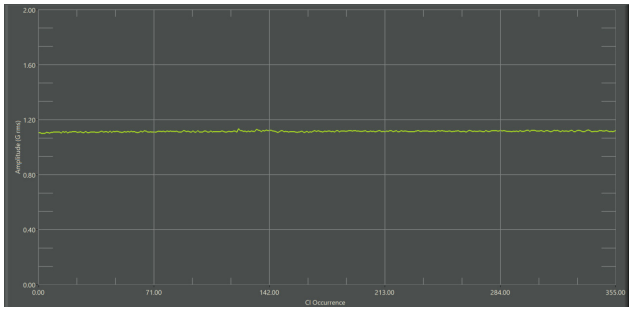

Figure 24: Software Image – CAN-MD® 3495A Accelerometer RMS Results

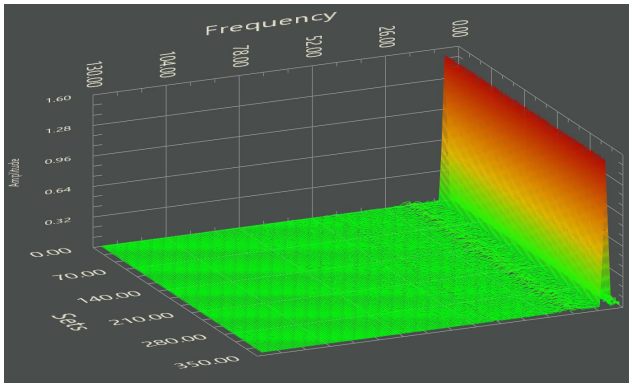

Figure 25: Software Image – CAN-MD® 3495A Accelerometer Waterfall Results

3.10 DIGITAL ACCELEROMETER – 3410A

The data obtained from the 3410A CAN-MD® Smart Accelerometer indicates no effect from the EMI in this test. Furthermore, the waterfall plot reveals no evidence of saturation throughout the entire frequency range examined. These results suggest that the 3410 accelerometer is highly resistant to the influence of EMI, reinforcing its reliability and stability in such environments.

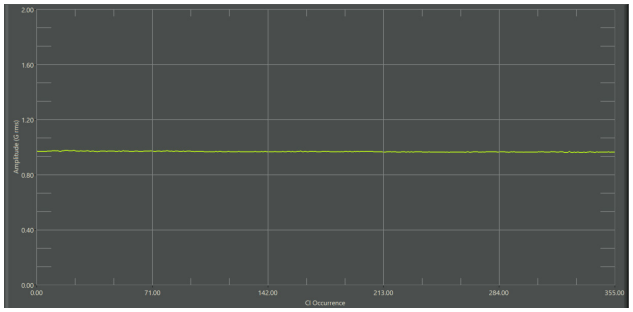

Figure 26: Software Image – CAN-MD® 3410A Accelerometer RMS Results

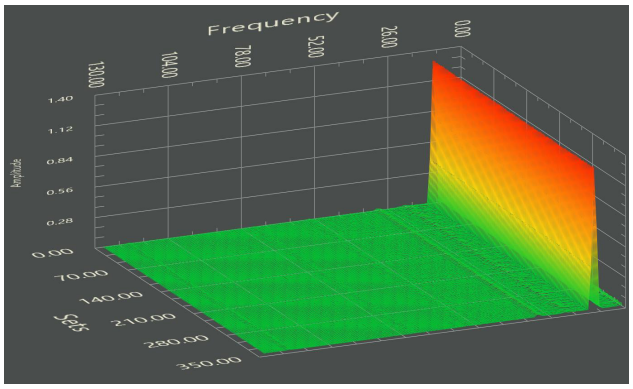

Figure 27: Software Image – CAN-MD® 3410A Accelerometer Waterfall Results

Dytran by HBK is a leading designer and manufacturer of innovative sensors, accelerometers, and associated electronics for measuringdynamic vibration, force and pressure. For over 40 years, Dytran has delivered sensing solutions that provide critical data toengineers in various industries. Dytran's broad product line includes high-quality uniaxial and triaxial piezoelectric and VC-MEMSaccelerometers, dynamic force and pressure transducers, and digital bus-based sensors. With a worldwide distribution network ofexperienced distributors in over seventy countries, Dytran prides itself on offering a first-class, concierge-level customer serviceexperience.

Visit www.hbkworld.com for additional information.

Dytran by HBK – Hottinger Brüel & Kjær
www.dytran.com
info@dytran.com